

A universal optical modulator for synthetic topologically tuneable structured matter

Chao He^{1,†,*}, Binguo Chen^{2,†}, Zipei Song^{1,†}, Zimo Zhao^{1,†}, Yifei Ma^{1,†}, Honghui He^{2,*}, Lin Luo^{3,*}, Tade Marozsak¹, An Wang¹, Rui Xu³, Peixiang Huang³, Xuke Qiu¹, Bangshan Sun¹, Jiahe Cui¹, Yuxi Cai¹, Yun Zhang^{4,5}, Patrick Salter¹, Julian AJ Fells¹, Ben Dai⁶, Shaoxiong Liu⁷, Limei Guo⁸, Hui Ma², Steve J Elston¹, Qiwen Zhan⁹, Chengwei Qiu¹⁰, Stephen M Morris¹, Martin J Booth¹, and Andrew Forbes¹¹

¹Department of Engineering Science, University of Oxford, Parks Road, Oxford, OX1 3PJ, UK

²Guangdong Research Center of Polarization Imaging and Measurement Engineering Technology, Institute of Biopharmaceutical and Health Engineering, Tsinghua Shenzhen International Graduate School, Tsinghua University, Shenzhen 518055, China

³College of Engineering, Peking University, Beijing 100871, China

⁴School of Archaeology, University of Oxford, South Parks Road, Oxford OX1 3TG, UK

⁵Institute of Archaeology, Chinese Academy of Social Sciences, Beijing 100101, China

⁶Department of Statistics, The Chinese University of Hong Kong, Shatin, HK SAR, China

⁷Shenzhen Sixth People's Hospital, Huazhong University of Science and Technology Union Shenzhen Hospital, 518052 Shenzhen, China

⁸Department of Pathology, School of Basic Medical Science, Peking University Health Science Center, Peking University Third Hospital, Beijing, China

⁹School of Optical-Electrical and Computer Engineering, University of Shanghai for Science and Technology, Shanghai 200093, China

¹⁰Department of Electrical and Computer Engineering, National University of Singapore, Singapore 117583, Singapore

¹¹School of Physics, University of the Witwatersrand, Private Bag 3, Johannesburg 2050, South Africa

[†]These authors contributed equally to this work

*Corresponding authors: chao.he@eng.ox.ac.uk; he.honghui@sz.tsinghua.edu.cn; luol@pku.edu.cn

Abstract (125 words)

Topologically structured matter, such as metasurfaces and metamaterials, have given rise to impressive photonic functionality, fuelling diverse applications from microscopy and holography to encryption and communication. Presently these solutions are limited by their largely static nature and preset functionality, hindering applications that demand dynamic photonic systems with reconfigurable topologies. Here we demonstrate a universal optical modulator that implements topologically tuneable structured matter as virtual pixels derived from cascading low functionality tuneable devices, altering the paradigm of phase and amplitude control to encompass arbitrary spatially varying retarders in a synthetic structured matter device. Our approach opens unprecedented functionality that is user-defined with high flexibility, allowing our synthetic structured matter to act as an information carrier, beam generator, analyser, and corrector, opening an exciting path to tuneable topologies of light and matter.

How light and matter interact has been a fundamental question for centuries and is still actively researched today, given renewed importance in the context of structured matter and structured light (1, 2). Unprecedented control of structured matter includes the creation of artificial atoms through metasurfaces and metamaterials, finding diverse applications in the control of light through linear (3) nonlinear (4), and quantum (5) enhancements. Topologically structured matter has emerged from condensed matter physics to imprint itself in the photonic domain, giving rise to topologically structured light fields (6) with textures in the polarisation and phase for vectorial light, optical skyrmions (7) and singular optical fields (8, 9). Light-matter interactions have also given rise to light as a probe, with structured light proving essential in unravelling complex systems; for instance, in rotational (10) and vectorial (11) metrology, chirality (12), and clinical diagnosis (13). In particular, topological protection and invariance are exciting avenues to explore in the context of light-matter interactions, with the promise of stable information transport and storage by imparting and detecting structure in light and matter. The transport of structured light through complex media is likewise highly topical and relevant in the field of communications (14) and biomedical imaging (13), and here crafting invariant forms of light or extending the notions of adaptive correction to arbitrary light forms is crucial (15, 16).

While there is a concerted drive towards tuneable and rewritable forms of structured matter (17, 18), topologically structured matter is presently limited by one or a combination of features such as preset and static functionality or limited tunability, hindering applications that demand dynamical photonic systems with complex tuneable topologies. The ubiquitous toolkit for dynamic control based on the use of spatial light modulator technology has so far been limited to the paradigm of complex amplitude modulation using the optical axis to impart phase changes (19) with liquid crystal devices (20) and digital micromirror device based approaches (21) being the most common. However, these techniques or other similar methods typically focus on the generation of structured light using well-defined polarisation (22) and are therefore of limited use in dynamic applications with varying inputs (13, 23). In recent years, there has also been an increasing trend in the use of tuneable devices such as metasurfaces and metamaterials to

achieve tuneable topological matter (17). Modern modulation techniques include free carrier density manipulation through electrical gating (24) and photocarrier excitation (25), micro-electro-mechanical (MEMS) technology (26, 27), magneto-optical control (28), dielectric environment modulation (29, 30), chemical approaches (31) and techniques exploiting optical nonlinearity (4). While these approaches offer versatility in certain applications such as beam steering (32), tuneable lenses (33) and dynamic holography (34), they still exhibit intrinsic limitations. These drawbacks encompass the limited range of modulation resulting in an inability to perform arbitrary vectorial field transformations and form structures like elliptical retarder arrays, limitations in spatial resolution and independent control in a pixelated manner and constraints that impede broader dynamic applications and the exploration of matter topology (7, 13, 23). On the rewritable front, optical modification of phase-changing materials has found great success in constructing reconfigurable structures (35, 36), but such techniques remain unable to exhibit dynamic behaviour necessary for general applications. Indeed, the highly flexible and complex forms of topologically structured matter for manipulating structured light require enhanced control not presently possible with those technologies and devices.

Here we overcome these vital limitations and demonstrate a universal light modulator that implements topologically tuneable structured matter synthesis as virtual pixels with unprecedented functionality even though they are derived from a cascade of low functionality devices, altering the paradigm of phase and amplitude control to encompass arbitrary spatially varying structured matter. We show that a cascade of elements with judicious encoding can mimic a pixel-controllable arbitrary retarder of any axis shape and orientation, retardance value as well as phase, simultaneously. We first show its power as a reconfigurable device to form novel liquid crystal based synthetic compound skyrmions, harnessing the anisotropic axis shape and orientation that the light sees, as an object-wise analogy to a Stokes vector field optical skyrmion. Different tuneable complex topologies such as skyrmion lattices and skyrmion bags are demonstrated to validate the feasibility. It can then be a beam generator by creating complex structured light, including optical skyrmions in high-order skyrmionic or bimeronionic formats (7). We demonstrate the topological protection of these dynamical states of light through both isotropic and anisotropic media. Next, we show the powerful capability of this modulator as a beam analyser by virtue of its ability to analyse all polarisation states simultaneously through providing complete analysing channels, exploiting the tuneability for enhancement in the flexibility of the detection through novel polar and cartesian optimization, both highly sample dependent. To show this, we use our analyser to experimentally probe biomedical and archaeological samples, which we validate against ground truth to quantitatively describe the fibrotic tissue and archaeological artefacts by their retardance profiles, enabling label-free optical sensing of bio-structures and sensitive materials. Finally, we show the dynamic correction of spatially varying arbitrary retardance aberration in both sensor-based and sensorless forms through a new object-wise adaptive optics approach, harnessing the ability to construct object-wise aberration correction, rather than the light-wise equivalent, which we demonstrate by correcting the focal spot of a complex aberrated optical system. To conclude, we discuss the extensibility of the scalable cascade to manipulate light further or form other complex structured matter. We believe these advances demonstrate the significant capability of this novel approach, unlocking the door to new tuneable topologies of light and matter.

Results

Concept. Tuneable digital technology (19) is an enabling tool for structured light but is restricted to simple amplitude and phase control for specific incident states of polarisation (SoP), while mapping of arbitrary input to arbitrary output in any spatial degree of freedom requires tuneable spatially varying retardance, presently only found in a non-tuneable form by sophisticated artificial atoms made from metasurfaces and metamaterials. Intriguingly, we can break this paradigm with the same technology that appears to prohibit it. At the heart of our approach is the notion of virtual pixels that mimic arbitrary retarders through a cascade of lower functionality devices (see Fig. 1a) such as spatial light modulators (SLMs) and/or deformable mirrors (DMs); for instance, four tuneable devices will simulate virtual pixels with four degrees of freedom, retarder geometry (α), orientation (β), retardance value (γ) and phase (δ), thus forming an arbitrary elliptical retarder (37–39), controlled by the four voltages applied to each low functionality device (see Method 1). The number of devices enable different functionality of these virtual pixels (see Fig. 1b, extended Figure 1, and Discussion) and can be seen as synthetic tuneable form of structured matter itself (see Discussion). We harness this synthetic structured matter for novel topological control of light and matter, as an information carrier, structured light generator, analyser, and corrector (see Fig. 1c), demonstrated through a wealth of applications and associated new methodologies.

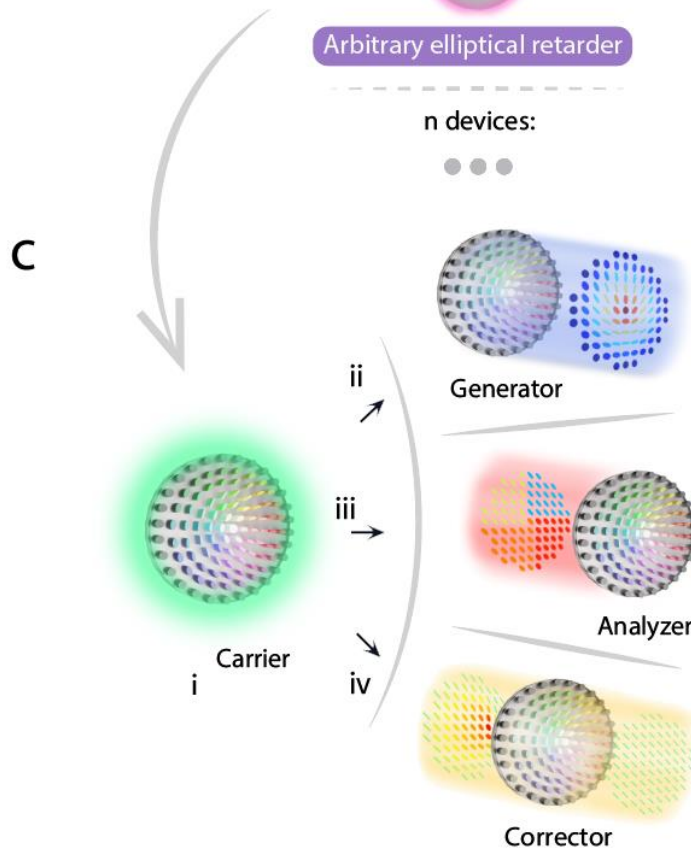
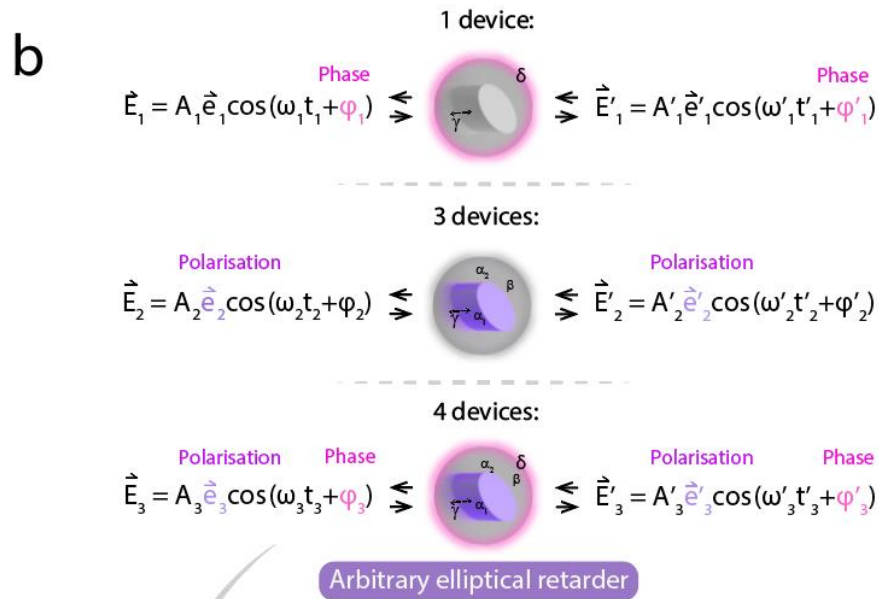
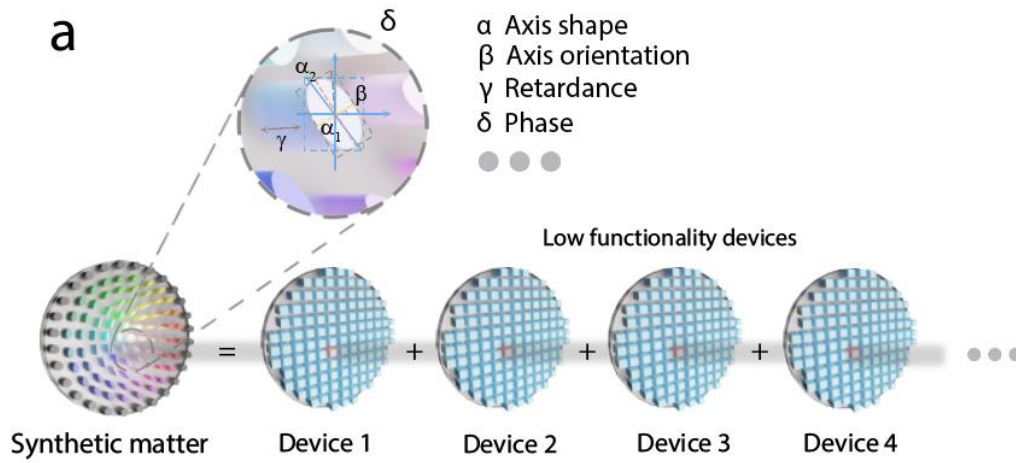


Fig. 1: **Synthetic topologically tuneable structured matter and its wide-range functionality.** (a) The matter and the synthetic virtual pixels. This illustration shows a universal optical modulator with the following controllable

parameters: axis geometry (α), orientation (β), retardance value (γ), phase (δ), and more. The optical modulator is formed by different numbers of cascaded low-functionality devices such as SLMs and DMs. (b) When the controllable parameters of the synthetic pixel increase, the functionalities of the matter will be enriched as well. The first row shows when δ or γ can be controlled, we can enable arbitrary phase-to-phase field conversion. The second row shows when α , β , and γ can be controlled, we can enable arbitrary polarisation-to-polarisation field conversion. The third row shows that based upon the second row, if an extra controllable parameter δ is added, then we can not only achieve arbitrary polarisation and phase field conversion, but also treat the pixel itself as an arbitrary elliptical retarder. More advanced parameter control and functionalities are discussed in the Discussion and Methods. (c) Roles that the matter can play when it becomes an arbitrary elliptical retarder: information carrier (i), beam generator (ii), beam analyser (iii) and beam corrector (iv).

Synthetic topological matter. Skyrmions have received considerable attention as an intriguing topologically protected information carrier (40–43). Figure 2 shows how the synthetic matter itself can act as a tuneable information carrier, forming new compound synthetic skyrmion fields with complex tuneable topologies. The principal idea is to harness the spatially varied elliptical axes field distribution of the arbitrary retarder array, analogous to the Stokes vector skyrmion in the light field (44) (Figs. 1a and 2b, and Method 2). To realise this, we construct our arbitrary retarder array using four tuneable devices, where the axis conditions (α and β) of the spatially distributed synthetic pixels are controlled by four voltages through a pre-determined mathematical relationship (see Method 1). Note here we set γ and δ as constant values for simplicity ($3\pi/2$ and 0). This enables us to write pre-determined information – e.g., complex skyrmions – into the axis field of the matter itself. By controlling the voltages, we encode different topologies including skyrmion lattices (Fig. 1c (i)), skyrmionium lattices (Fig. 1c (ii)), skyrmion bags (Fig. 1d (iii)), and high-order skyrmion bags (Fig. 1d (iv)) sequentially into the matter; and decode it through an imaging Mueller matrix polarimeter to decompose the elliptical axis distributions from the sequentially obtained images. From the results and corresponding theoretical patterns shown in Figs. 2c and 2d, it is easy to observe that the pre-determined information can be encoded and decoded effectively. To the best of our knowledge, we have not only encrypted novel formats of synthetic skyrmions, but also for the first time achieved complex skyrmion topologies through tuneable optical retarders. We note that at this stage, the elliptical retarder array resembles a cascaded linear birefringent array, hence the complex skyrmions appear from the beam’s point of view, as a synthetic structure. However, this preliminary validation highlights the potential significance of creating a spatially variant authentic elliptical retarder in a single device, which will pave the way for novel opportunities to create tuneable skyrmions in materials, offering substantial avenues for further exploration.

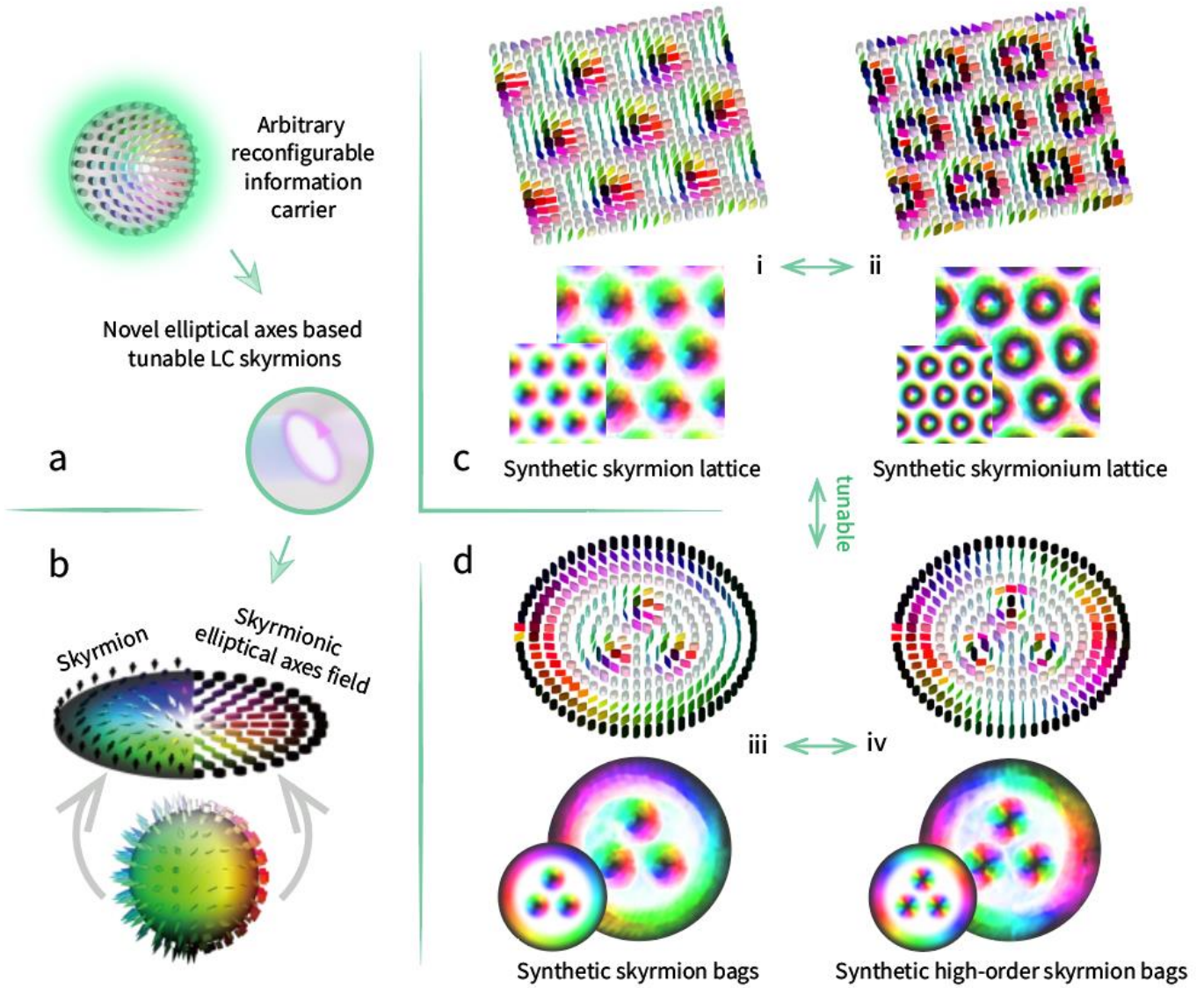


Fig. 2: **Synthetic matter as an information carrier.** (a) The elliptical axes of the arbitrary retarders act as a new basis for generating skyrmions (see Method 2). (b) Demonstration of one-to-one mapping between a half skyrmionic field and a half axis based skyrmionic field. (c) and (d) exemplify the tuneability of the synthetic matter to generate compound synthetic skyrmions with complex topologies including skyrmion lattices (i), skyrmionium lattices (ii), skyrmion bags (iii), and high-order skyrmion bags (iv). In each scenario, the sub-figure at the top shows the spatially varying elliptical axes field with fixed retardance values (see extended Figure 2), and the ones below show simulated and experimentally achieved skyrmionic fields that are probed by the light beam. The hue colorbar refers to Ref (7).

Structured light generator. To demonstrate the broad scope of methodologies and applications that the synthetic retarder matter can enable, we utilise it as a new skyrmionic beam generator by taking advantage of the virtual topological structure of the device to create topological forms of structured light. Optical skyrmions are topologically protected quasiparticles that have been recently introduced to the field of structured light (7). However, methods of generating optical skyrmions are still in their infancy, hindering the realisation of tuneable complex topology. To address this problem, we demonstrate new light manipulation capabilities through our synthetic matter. The procedure of generating complex skyrmionic beams is as follows: First, a field with known polarisation and phase is incident upon the matter. Here we use a beam with uniform circular polarisation and a flat phase for simplicity. Second, as a key demonstration we choose the expected output field to be either a high-order skyrmionic beam or a bimeroniumic beam (Fig. 3a). Third, we calculate the corresponding spatial retarder distributions (different α , β , and γ values; δ set as flat) and encode them into the matter (see Method 1); fourth, we use a Stokes polarimeter to record the beam profiles and a Mueller polarimeter to obtain the properties of the matter for further analysis. Both the theoretical and experimental results can be found in Figs. 3a and 3b. It can be appreciated that the complex skyrmionic beams generated by our synthetic matter, which has not been shown before, are well matched to their corresponding ground truth. The formation of virtually pixelated retarders enables beam manipulation with unprecedented precision

and flexibility, and more broadly circumvent the restriction of needing to pre-determine the input SoP and phase (see Method 1). Moreover, any complex topology can theoretically be realised using synthetic matter through the same procedure.

To investigate the performance of providing topological protection for both beams, we assembled a complex beam probing system (Fig. 3c) comprising different perturbations M1 (isotropic) and M2 (anisotropic). For M1, a uniform few-micron thick water layer was sandwiched between two thin glass slides; and for M2, an unknown waveplate was used. In terms of M1, we first illuminated the media with two beams sequentially, alongside moving the slide laterally such that the beam hits the slide at six random locations. The beam profiles were then recorded by a Stokes polarimeter and a camera after the media. Corresponding results are given in the upper row of Fig. 3d. The two input beam profiles are displayed on the left of the plot, and the plot itself shows how the calculated output beam topological number (y-axis) and field profile varies at each of the six slide locations (x-axis). Results with respect to M2 after similar experimental procedures are given in the lower row of Fig. 3d, with the only difference of randomly changing to six different waveplate axis conditions rather than moving the waveplate laterally. These experimental results demonstrate the topological protection of these complex fields by virtue of a constant skyrmion number before and after propagation through both isotropic and anisotropic media (see mathematical proof in Method 3; more data in extended Figure 3), which further validates how our structured matter paves the way for advanced tuneable structured light generation and importantly, towards future robust optical communication approaches.

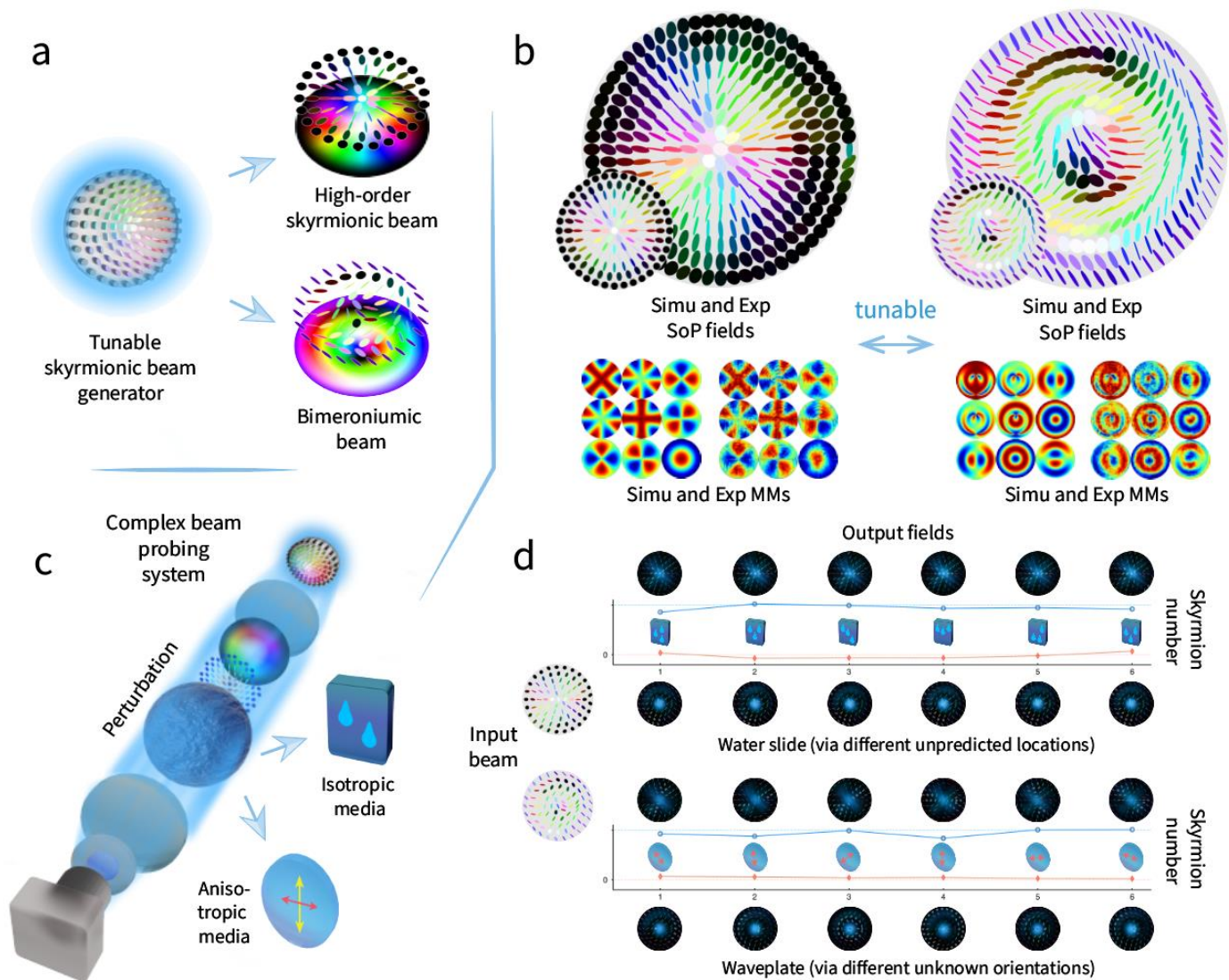


Fig. 3: Synthetic matter as a beam generator. (a) Structured matter acts as a tuneable beam generator, for high-order skyrmionic beam and bimerioniumic beam generation. (b) Experimental Stokes vector and intensity fields of the generated skyrmionic and bimerioniumic beam, as well as the Mueller matrices of the corresponding matter that generated them. Different ellipses and colours represent different Stokes vectors (refer to Ref (7)). (c) A complex beam probing system with different perturbations – isotropic media M1 (water slide) and anisotropic media M2 (waveplate). During the proof-of-concept experiments, the output beams were recorded by a Stokes polarimeter to characterize the spatially varying SoP and a camera was used to record the focal spots. (d) The upper row shows how the calculated

skyrmionic numbers of both output beams varied when they hit M1 at six different locations. The lower row represents the results from using M2 under the same experimental process, with the only difference of using six unknown waveplate axis orientations rather than random regions of the waveplate.

Optical polarisation analyser. The synthetic virtual pixels of the matter can serve as tuneable polarisation analysing channels. The tunability of the analysing channel is important, as different applications require different optimisation strategies for SoP sensing (13). For instance, in certain pathological imaging scenarios, the measurement precision of circular SoP is more important than its linear counterpart (45), while linear SoP is given more consideration in certain material characterisation applications (46). Taking advantage of its unique property to analyse all SoPs simultaneously, Full Poincaré units (FPU) (47) can provide different optimisation strategies (see Method 4) and can be used to achieve high-precision polarisation measurement through physical inference, circumventing the error accumulation problem of traditional measurement processes (47). However, the realisation of reconfigurable FPUs is limited by the restriction of existing devices as they are all passive. Our synthetic matter breaks such restrictions by forming different FPUs with tuneable optimisation states – Polar optimisation (PO) and Cartesian optimisation (CO) configurations – through different retarder distributions. The former is optimised for circularly polarised light, while the latter is optimised for linear SoPs (see Method 4).

To realize a tuneable FPU that consists of all linear retardance values and axis orientations, we encode different spatially varying linear retarder distributions (47) into the matter (different distributions of α , β , γ and δ ; see Fig. 4a and Method 1). To validate the feasibility of the tuneable FPU device, a polarisation scanning system is adopted (Fig. 4b), where the matter and a fixed polariser form the polarisation state analyser (PSA). This configuration enables proof-of-concept experiments on the characterisation of a biomedical sample and an archaeological sample via PO and CO configurations, respectively. The procedure proceeds as follows: first, we measured the Mueller matrices of the matter in both PO and CO configurations to ensure that the matter is of expected formation. The results alongside theory are presented in Figs. 4c and 4d; second, we used PO for biomedical sensing and CO for archaeological sample characterisation, under circular SOP illumination. The acquired polarimetric images of the targets (Stokes vector images) and their statistical analysis are presented in Figs. 4c and 4d. These metrics or their combinations can potentially be used to reveal differences between fibrosis and non-fibrosis or regions with different crystallisation levels. Finally, decomposed retardance values Δ under those configurations (45) are also provided to compare with ground truth Δ' taken by traditional polarisation microscopes (48). We can see that the PO method can differentiate fibrosis/non-fibrosis regions through their retardance values and they match well with the ground truth, as does the CO method for quantitatively describing the crystallisation condition inside the sample. Our synthetic matter provides a novel routine for tuneable FPU-based polarisation sensing towards various applications. For more data analysis, see extended Figure 4.

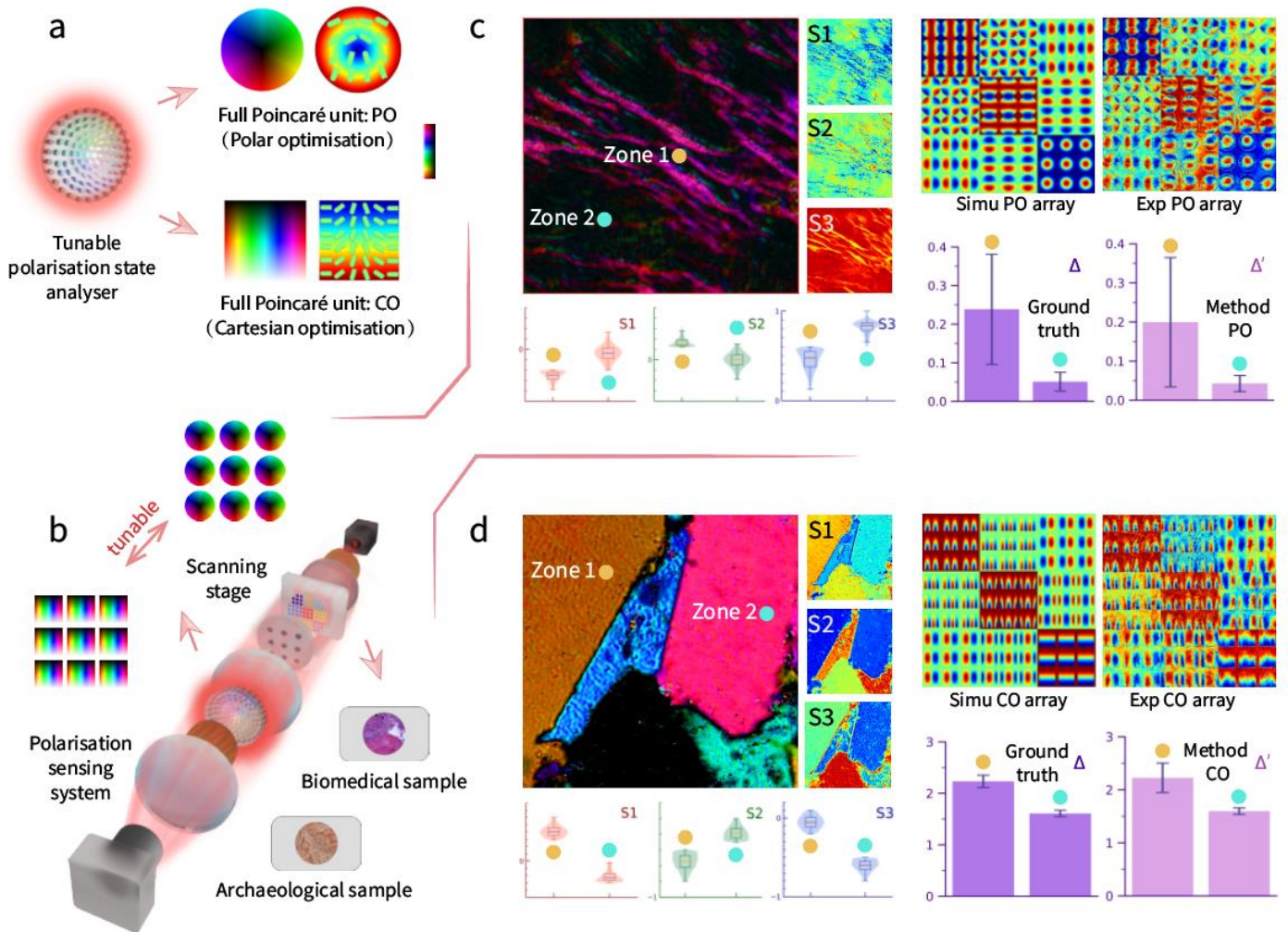


Fig. 4: **Synthetic matter as an optical analyser.** (a) Structured matter acts as a tuneable PSA. It can form patterned retarder array distributions for PO and CO configurations (see Methods 4). (b) A scanning polarimetric imaging system with a tuneable PSA that can change from PO to CO (or vice versa) to meet different sensing requirements. Biomedical or archaeological samples are tested to validate the feasibility. (c) An example of analysing the fibrosis process inside a biomedical sample using PO optimisation. The retardance image, as well as the associated Stokes vector images, are given. Regions Zone 1 and Zone 2 in the retardance image are chosen for quantitative comparisons of components S_1 , S_2 , and S_3 , as well as statistical comparisons between the tested δ value and the ground truth. Mean value and variance are given. The Mueller matrix of the PO array is shown by simulation and experimental results. (d) An example of analysing the crystallisation properties of an archaeological sample using CO optimisation. Similar images and quantitative analysis are given in sub-figures. The brown and blue circles represent data from Zone 1 and Zone 2, respectively.

Vectorial aberration corrector. Besides being an information carrier, beam generator and beam analyser, through constructing arbitrary retarders the matter can act as a novel dynamic aberration corrector for adaptive optics (AO). AO is a powerful technique that has been of benefit in various modern optical systems from astronomical telescopes to super-resolution microscopes (13, 23). To meet the high demand of rapidly developing vectorial optics and photonics, AO techniques that address both polarisation and phase correction have been recently introduced (16), with broad applications spanning from vectorial optical communications to vector-sensitive imaging methods. Polarisation aberrations, which are described using Jones or Mueller matrices (MM), lead to complex matrix calculation induced errors that cannot yet be eliminated when calculating the vectorial field patterns for aberration compensation (16). One possible route is to form an complementary spatially varying polarisation aberrated media such that the combined media is polarisation insensitive (for instance, a retarder with $2k\pi$ retardance value, which has no impact on the SoP). However, to the best of our knowledge, this is not readily achievable using any kind of existing device. By taking advantage of the synthetic matter's tuneable functionality to act as an arbitrary retarder array, we can create the 'complementary object' in a pixelated manner, thus enabling a new object-wise AO technique (we named it O-AO) using such a new corrector. Two novel AO methods are therefore presented in the O-AO regime, enabled by the novel corrector sensorbased- and sensorless-AO (see Fig. 5a), derived from the corresponding

conventional AO methods. To validate their feasibility, an aberrated focusing system (see Fig. 5b) was used for proof-of-concept demonstrations.

Experimental procedures for validation of sensorbased O-AO are as follows: First, an external polarisation aberration was introduced into the system (a tilted waveplate array (16)). Second, an MM sensor was used to measure the existing aberration. Third, an complementary retarder was formed using the synthetic matter (controlled by α , β , γ and δ values) to finish the compensation. Detailed procedures are described in Method 5 and extended Figure 5. Fourth, we ran sensorbased phase AO correction (49) to compensate for the residual phase errors. Fig. 5c shows the MMs of the system before (O-AO off) and after correction (O-AO on). The four phase patterns on the cascaded devices, the intensity profile of the focal spots, as well as the cross-section of the focal spots are also given in Fig. 5c. We can observe that the MM was recovered into a diagonal MM (equivalent to a full waveplate MM which is SoP insensitive) as expected, and the beam profile as well as the intensity value both increased after the correction process. Validation of sensorless O-AO (without an MM sensor) was also conducted, by optimising the focus intensity to find the best compensation. To estimate the polarisation aberration, we harnessed a novel set of object-wise modes similar to Zernike modes that we name retardance modes (see Method 5). These modes can be used to manipulate the retardance distribution on the synthetic matter in a pixel-wise manner following a sensorless AO approach (i.e., applying different Zernike modes on the corrector using different parameters, recording focal spot images sequentially). After adopting different retardance modes, the set of images provided information that enabled estimation of the retardance aberrations, which was then used to drive the corrector (details see Method 5, extended Figures 6 and 7). The final phase patterns on the corrector devices, the intensity profile of the focal spots, as well as the beam cross-section of the focal spots are shown in Fig. 5d, similar to the case of the sensorbased method. A fitted curve of one of the retardance modes – piston, is also illustrated. Note that in conventional AO, piston normally does not change the profile of the focal spot and thus is usually neglected (49). However, here the piston mode represents the retardance value of the object, which changes the overall retarder performance and thus affects the focal spot. To the best of our knowledge, this is the first time the concept of AO correction is expanded from the light domain to the matter domain – i.e., rather than just correcting a state of light, we are compensating a state of retardance, which is significantly important as it implements a direct matter-to-matter compensation approach. Hence the compensation is valid for all possible input vectorial states, and is not restricted to a particular output state. The techniques are expected to benefit applications including galaxy detection, lithographic or laser-based nanofabrication, as well as clinical diagnosis.

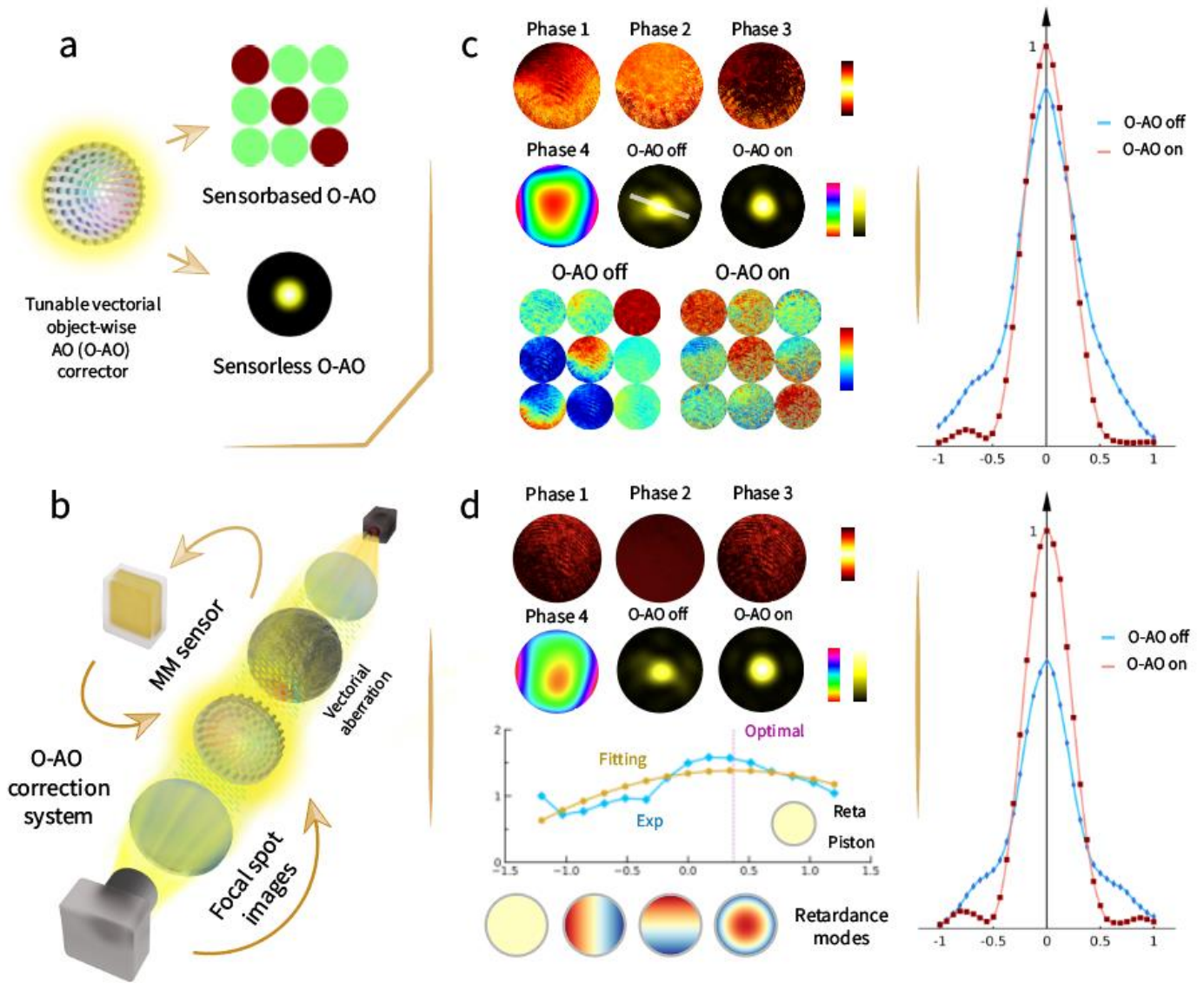


Fig. 5: **Synthetic matter as a beam corrector.** (a) Structured matter acts as a tuneable object-wise AO corrector, which can conduct both sensorbased- and sensorless O-AO correction. (b) An aberrated optical focussing system with an O-AO corrector to validate sensorbased (through an MM polarimeter) and sensorless (through focal spot images) O-AO methods. (c) Results for sensorbased O-AO off vs. on. Phase patterns on all four devices after O-AO correction, foci profiles, MMs, as well as sampled focal spot cross-sections (white line on the focal spot image) before and after correction are presented. The vectorial aberration is a tilted waveplate array (16). (d) Results for sensorless O-AO off vs. on for the same retardance aberration in (c). Phase patterns on all four devices after O-AO correction, foci profiles, as well as sampled focal spot cross-sections (white line on the focal spot image) before and after correction are presented. A fitted curve for retardance piston mode is also given.

Discussion and conclusion

Our results show that the synthetic structured matter (demonstrated in this work by tuneable arbitrary retarders) enables various novel dynamic optical methods and applications. Proof-of-concept demonstrations validate how the synthetic matter can be effectively used as an information carrier (dynamic tunability), beam generator (dynamic topological beams), analyser (dynamic target optimisation), and corrector (dynamic correction). Carrier: previous liquid crystal skyrmions are based on harnessing patterned director orientations to encode information, and the consequent skyrmions have limited tuneability and flexibility. In addition, the directors need to wrap twice to cover the full sphere and form the skyrmionic structures. We now enrich the liquid crystal skyrmion community by introducing a new set of axes geometry based skyrmions (currently in a compound synthetic way). It now can cover the full 2-sphere in a similar way to the Stokes vector can conduct, and generate tuneable structures via optical encoding and decoding processes, forming a strong basis for new insights spanning from data storage to cryptography. Generator: traditional skyrmion generators still focus on the paradigm of phase and amplitude modulation or pre-set functionalities of the devices, hindering the quality and capacity of the generated skyrmionic beams. Now utilising our synthetic matter, it is expected that complex skyrmionic beams with more controllable topologies, or in a novel format

such as a topological beam array, can be achieved in a tuneable manner. This synthetic matter approach may open new avenues for modern dynamic complex beam probing, or optical communications via enriched channel numbers and capabilities. Analyser: the matter in effect provides a tuneable platform of arbitrary polarisation analysis channels, which cannot be constructed with any existing device. It further paves the way for novel optimisation geometries, for example, elliptical SoP based, or hybrid states determined by the specific application. Corrector: previous AO methods all focus on the manipulation of the light beam, while our synthetic matter pushes AO techniques into a new domain that directly manipulates the property of matter to compensate for the full vectorial aberrating properties of an object, rather than simply correcting for a single output state. Future work could focus on more sophisticated vectorial modes, that either use the retardance value, or the axis shape and orientation, or hybrid combinations. Implementations may benefit various research areas such as direct laser writing techniques and lithography.

This work has focused so far on the potential application of the structured matter in the format of an arbitrary retarder, but its potential functionalities can be further enhanced by cascading more low functionality devices. Fig. 6 conceptually illustrates the formation of more complex structured matter with intensity and time control (in effect, to control different degrees of polarisation), although the former one would need an extra control mechanism of the power and the latter one has been solely demonstrated before (50). More broadly, the synthetic matter itself also features great potential to form other complex structured matter such as tuneable diattenuators or depolarisers. More discussion on the realisation of such matter through adding extra devices can be found in Methods 6, 7, 8, and extended Figure 8. Overall, our tuneable structured matter is expected to play an important role in the modern optics community, especially in the fields of dynamic and vectorial optics and photonics, to address recent demands of modern optical communication, optical sensing/imaging, adaptive optics, optics skyrmions and beyond.

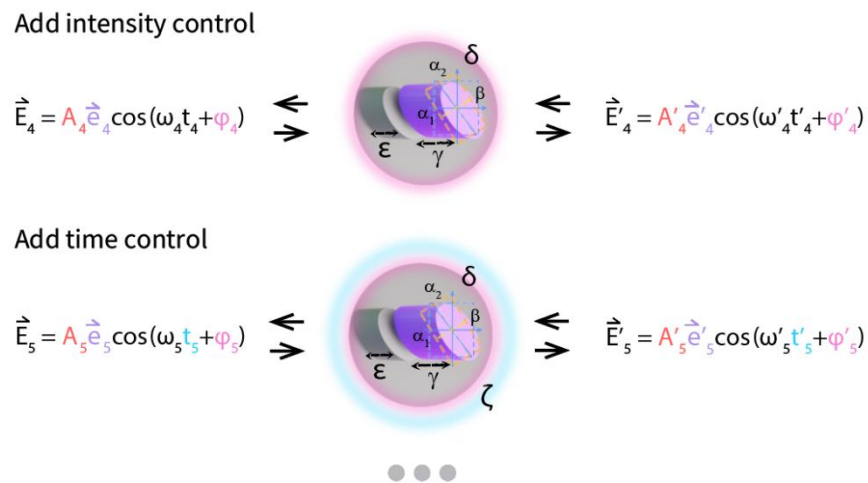


Fig. 6: **Extended functionalities of the synthetic matter approach.** By adding more devices, the matter would be able to manipulate the intensity values as well as the degrees of polarisation (through time control), as well as enriching its own vectorial properties. The ϵ and ζ in the figure present attenuation value and depolarisation value. The manipulation mechanism and further discussion can be found in Methods 6, 7, 8 and extended Figure 8.

Acknowledgments

C.H. who led this research was supported through a Junior Research Fellowship from St John's College, University of Oxford. The authors also thank the Engineering and Physical Sciences Research Council (UK) (EP/R004803/01) (P.S.S.); the European Research Council (AdOMiS, no. 695140) (C.H. and M.J.B.); NSFC 92050202 (Q.Z.); Shenzhen Key Fundamental Research Project (No. JCYJ20210324120012035) (H.H.).

Competing interests

The authors declare no competing interests.

Additional Information

Correspondence and request for materials should be addressed to C.H., H.H., or L.L.

Reference

1. N. M. Litchinitser, Structured light meets structured matter. *Science* **337**, 1054–1055 (2012).
2. A. Forbes, M. de Oliveira, M. R. Dennis, Structured light. *Nat Photonics* **15**, 253–262 (2021).
3. S. B. Glybovski, S. A. Tretyakov, P. A. Belov, Y. S. Kivshar, C. R. Simovski, Metasurfaces: From microwaves to visible. *Phys Rep* **634**, 1–72 (2016).
4. G. Li, S. Zhang, T. Zentgraf, Nonlinear photonic metasurfaces. *Nat Rev Mater* **2**, 1–14 (2017).
5. A. S. Solntsev, G. S. Agarwal, Y. S. Kivshar, Metasurfaces for quantum photonics. *Nat Photonics* **15**, 327–336 (2021).
6. Y. Shen, X. Wang, Z. Xie, C. Min, X. Fu, Q. Liu, M. Gong, X. Yuan, Optical vortices 30 years on: OAM manipulation from topological charge to multiple singularities. *Light Sci Appl* **8**, 90 (2019).
7. Y. Shen, Q. Zhang, P. Shi, L. Du, A. V. Zayats, X. Yuan, Topological quasiparticles of light: optical skyrmions and beyond. *arXiv preprint arXiv:2205.10329* (2022).
8. E. Otte, C. Alpmann, C. Denz, Polarization singularity explosions in tailored light fields. *Laser Photon Rev* **12**, 1700200 (2018).
9. X. Wang, Z. Li, Y. Gao, Z. Yuan, W. Yan, Z.-C. Ren, X.-L. Wang, J. Ding, H.-T. Wang, Configuring polarization singularity array composed of C-point pairs. *IEEE Photonics J* **14**, 1–6 (2022).
10. M. P. J. Lavery, F. C. Speirits, S. M. Barnett, M. J. Padgett, Detection of a spinning object using light's orbital angular momentum. *Science* **341**, 537–540 (2013).
11. L. Fang, Z. Wan, A. Forbes, J. Wang, Vectorial doppler metrology. *Nat Commun* **12**, 4186 (2021).
12. M. Hanifeh, M. Albooyeh, F. Capolino, Optimally chiral light: Upper bound of helicity density of structured light for chirality detection of matter at nanoscale. *ACS Photonics* **7**, 2682–2691 (2020).
13. C. He, H. He, J. Chang, B. Chen, H. Ma, M. J. Booth, Polarisation optics for biomedical and clinical applications: a review. *Light Sci Appl* **10**, 194 (2021).
14. I. Nape, K. Singh, A. Klug, W. Buono, C. Rosales-Guzman, A. McWilliam, S. Franke-Arnold, A. Kritzinger, P. Forbes, A. Dudley, Revealing the invariance of vectorial structured light in complex media. *Nat Photonics* **16**, 538–546 (2022).
15. C. He, Y. Shen, A. Forbes, Towards higher-dimensional structured light. *Light Sci Appl* **11**, 205 (2022).
16. C. He, J. Antonello, M. J. Booth, Vectorial adaptive optics. *eLight* **3** (2023).
17. A. M. Shaltout, V. M. Shalaev, M. L. Brongersma, Spatiotemporal light control with active metasurfaces. *Science* **364**, eaat3100 (2019).
18. A. H. Dorrah, F. Capasso, Tunable structured light with flat optics. *Science* **376**, eabi6860 (2022).
19. Y. Yang, A. Forbes, L. Cao, A review of liquid crystal spatial light modulators: devices and applications. *Opto-Electronic Science*, 230021–230026 (2023).
20. A. H. Dorrah, M. Zamboni-Rached, M. Mojahedi, Experimental demonstration of tunable refractometer based on orbital angular momentum of longitudinally structured light. *Light Sci Appl* **7**, 40 (2018).

21. C. Rosales-Guzmán, X.-B. Hu, A. Selyem, P. Moreno-Acosta, S. Franke-Arnold, R. Ramos-Garcia, A. Forbes, Polarisation-insensitive generation of complex vector modes from a digital micromirror device. *Sci Rep* **10**, 10434 (2020).
22. W. Han, Y. Yang, W. Cheng, Q. Zhan, Vectorial optical field generator for the creation of arbitrarily complex fields. *Opt Express* **21**, 20692–20706 (2013).
23. M. J. Booth, Adaptive optical microscopy: the ongoing quest for a perfect image. *Light Sci Appl* **3**, e165 (2014).
24. G. Kafaie Shirmanesh, R. Sokhoyan, R. A. Pala, H. A. Atwater, Dual-gated active metasurface at 1550 nm with wide (> 300) phase tunability. *Nano Lett* **18**, 2957–2963 (2018).
25. L. Cong, Y. K. Srivastava, H. Zhang, X. Zhang, J. Han, R. Singh, All-optical active THz metasurfaces for ultrafast polarization switching and dynamic beam splitting. *Light Sci Appl* **7**, 28 (2018).
26. E. Arbabi, A. Arbabi, S. M. Kamali, Y. Horie, M. Faraji-Dana, A. Faraon, MEMS-tunable dielectric metasurface lens. *Nat Commun* **9**, 812 (2018).
27. C. Meng, P. C. V Thrane, F. Ding, S. I. Bozhevolnyi, Full-range birefringence control with piezoelectric MEMS-based metasurfaces. *Nat Commun* **13**, 2071 (2022).
28. D. O. Ignatyeva, D. M. Krichevsky, V. I. Belotelov, F. Royer, S. Dash, M. Levy, All-dielectric magneto-photonic metasurfaces. *J Appl Phys* **132** (2022).
29. S.-Q. Li, X. Xu, R. Maruthiyodan Veetil, V. Valuckas, R. Paniagua-Domínguez, A. I. Kuznetsov, Phase-only transmissive spatial light modulator based on tunable dielectric metasurface. *Science* **364**, 1087–1090 (2019).
30. A. Komar, R. Paniagua-Domínguez, A. Miroschnichenko, Y. F. Yu, Y. S. Kivshar, A. I. Kuznetsov, D. Neshev, Dynamic beam switching by liquid crystal tunable dielectric metasurfaces. *ACS Photonics* **5**, 1742–1748 (2018).
31. R. Kaissner, J. Li, W. Lu, X. Li, F. Neubrech, J. Wang, N. Liu, Electrochemically controlled metasurfaces with high-contrast switching at visible frequencies. *Sci Adv* **7**, eabd9450 (2021).
32. Y.-Y. Xie, P.-N. Ni, Q.-H. Wang, Q. Kan, G. Briere, P.-P. Chen, Z.-Z. Zhao, A. Delga, H.-R. Ren, H.-D. Chen, Metasurface-integrated vertical cavity surface-emitting lasers for programmable directional lasing emissions. *Nat Nanotechnol* **15**, 125–130 (2020).
33. Z. Han, S. Colburn, A. Majumdar, K. F. Böhringer, MEMS-actuated metasurface Alvarez lens. *Microsyst Nanoeng* **6**, 79 (2020).
34. J. Li, S. Kamin, G. Zheng, F. Neubrech, S. Zhang, N. Liu, Addressable metasurfaces for dynamic holography and optical information encryption. *Sci Adv* **4**, eaar6768 (2018).
35. L. Jiang, A.-D. Wang, B. Li, T.-H. Cui, Y.-F. Lu, Electrons dynamics control by shaping femtosecond laser pulses in micro/nanofabrication: modeling, method, measurement and application. *Light Sci Appl* **7**, 17134 (2018).
36. K. Chaudhary, M. Tamagnone, X. Yin, C. M. Spägle, S. L. Oscurato, J. Li, C. Persch, R. Li, N. A. Rubin, L. A. Jauregui, K. Watanabe, T. Taniguchi, P. Kim, M. Wuttig, J. H. Edgar, A. Ambrosio, F. Capasso, Polariton nanophotonics using phase-change materials. *Nat Commun* **10**, 4487 (2019).
37. Q. Hu, C. He, M. J. Booth, Arbitrary complex retarders using a sequence of spatial light modulators as the basis for adaptive polarisation compensation. *Journal of Optics* **23**, 065602 (2021).
38. R. Chipman, W. S. T. Lam, G. Young, *Polarized Light and Optical Systems* (CRC press, 2018).
39. A. Sit, L. Giner, E. Karimi, J. S. Lundeen, General lossless spatial polarization transformations. *Journal of Optics* **19**, 094003 (2017).
40. A. Fert, N. Reyren, V. Cros, Magnetic skyrmions: advances in physics and potential applications. *Nat Rev Mater* **2**, 1–15 (2017).
41. D. Foster, C. Kind, P. J. Ackerman, J.-S. B. Tai, M. R. Dennis, I. I. Smalyukh, Two-dimensional skyrmion bags in liquid crystals and ferromagnets. *Nat Phys* **15**, 655–659 (2019).
42. M. Król, H. Sigurdsson, K. Rechcińska, P. Oliwa, K. Tyszka, W. Bardyszewski, A. Opala, M. Matuszewski, P. Morawiak, R. Mazur, W. Piecek, P. Kula, P. G. Lagoudakis, B. Piętka, J. Szczytko, Observation of second-order meron polarization textures in optical microcavities. *Optica* **8**, 255–261 (2021).
43. S. Donati, L. Dominici, G. Dagvadorj, D. Ballarini, M. De Giorgi, A. Bramati, G. Gigli, Y. G. Rubo, M. H. Szymańska, D. Sanvitto, Twist of generalized skyrmions and spin vortices in a polariton superfluid. *Proceedings of the National Academy of Sciences* **113**, 14926–14931 (2016).
44. S. Gao, F. C. Speirits, F. Castellucci, S. Franke-Arnold, S. M. Barnett, J. B. Götte, Paraxial skyrmionic beams. *Phys Rev A* **102**, 053513 (2020).
45. J. Chang, H. He, Y. Wang, Y. Huang, X. Li, C. He, R. Liao, N. Zeng, S. Liu, H. Ma, Division of focal plane polarimeter-based 3×4 Mueller matrix microscope: a potential tool for quick diagnosis of human carcinoma tissues. *J Biomed Opt* **21**, 56002 (2016).
46. Z. Zhao, B. Chen, P. S. Salter, M. J. Booth, D. O'Brien, S. J. Elston, S. M. Morris, Multielement Polychromatic 2D Liquid Crystal Dammann Gratings. *Adv Mater Technol* **8**, 2200861 (2023).

47. C. He, J. Lin, J. Chang, J. Antonello, B. Dai, J. Wang, J. Cui, J. Qi, M. Wu, D. S. Elson, Full Poincaré polarimetry enabled through physical inference. *Optica* **9**, 1109–1114 (2022).
48. H. He, R. Liao, N. Zeng, P. Li, Z. Chen, X. Liu, H. Ma, Mueller matrix polarimetry—an emerging new tool for characterizing the microstructural feature of complex biological specimen. *Journal of Lightwave Technology* **37**, 2534–2548 (2019).
49. K. M. Hampson, R. Turcotte, D. T. Miller, K. Kurokawa, J. R. Males, N. Ji, M. J. Booth, Adaptive optics for high-resolution imaging. *Nature Reviews Methods Primers* **1**, 68 (2021).
50. D. Marco, G. López-Morales, M. del M. Sánchez-López, Á. Lizana, I. Moreno, J. Campos, Customized depolarization spatial patterns with dynamic retardance functions. *Sci Rep* **11**, 9415 (2021).